A Heating-Superfusion Platform Technology for Single Cell Investigations.

ARTICLE *in* ANALYTICAL CHEMISTRY · DECEMBER 2014

Impact Factor: 5.64 · DOI: 10.1021/ac5031418 · Source: PubMed

5 AUTHORS, INCLUDING:

Shijun Xu

Chalmers University of Technology

7 PUBLICATIONS **9** CITATIONS

SEE PROFILE

Alar Ainla

Harvard University

20 PUBLICATIONS **147** CITATIONS

SEE PROFILE

Gavin D. M. Jeffries

Chalmers University of Technology

44 PUBLICATIONS **1,182** CITATIONS

SEE PROFILE

analytical chemistry

Technical Note

pubs.acs.org/ac

A Heating-Superfusion Platform Technology for the Investigation of Protein Function in Single Cells

Shijun Xu,[†] Alar Ainla,[§] Kent Jardemark,[‡] Aldo Jesorka,[†] and Gavin D. M. Jeffries*[,†]

[†]Department of Chemical and Biological Engineering, Chalmers University of Technology Kemivägen 10, SE-412 96 Gothenburg, Sweden

[‡]Department of Physiology and Pharmacology, Karolinska Institutet, SE-17177 Stockholm, Sweden

[§]Department of Chemistry and Chemical Biology, Harvard University, Cambridge, Massachusetts 02138, United States

Supporting Information

ABSTRACT: Here, we report on a novel approach for the study of single-cell intracellular enzyme activity at various temperatures, utilizing a localized laser heating probe in combination with a freely positionable microfluidic perfusion device. Through directed exposure of individual cells to the pore-forming agent α-hemolysin, we have controlled the membrane permeability, enabling targeted delivery of the substrate. Mildly permeabilized cells were exposed to fluorogenic substrates to monitor the activity of intracellular enzymes, while adjusting the local temperature surrounding the target cells, using an infrared laser heating system. We generated quantitative estimates for the intracellular alkaline phosphatase activity at five different temperatures in different cell lines, constructing temperature-response curves of enzymatic activity at the single-cell level. Enzymatic activity was determined rapidly after cell permeation, generating five-point temperature-response curves within just 200 s.

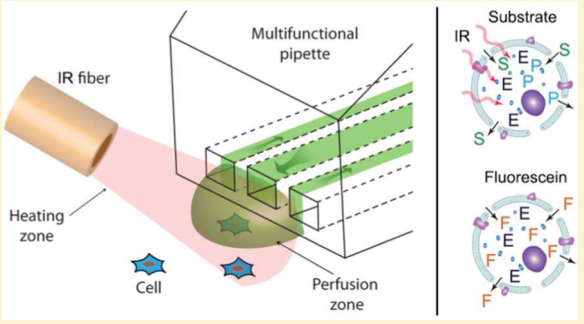

In biology, unraveling the kinetics and complexities of protein activity within cells has been a prevalent task for many years.[1] Enzymes, which are a key family of proteins, are important biological components within cells and are involved in all major cellular processes, including transcription and translation of genes, ATP conversion, and protein synthesis. Although we have a fine understanding of many biological processes, from traditional biochemical and biophysical experiments (e.g., enzymatic inhibition, metabolic pathways, and structural basis of enzymes),[2] there is a lack of understanding of the functional and kinetic aspects of enzymes in their natural milieu.[3,4] The intrinsic limitation of traditional methods leads to an incomplete understanding of the functional aspects of enzymes, since key intracellular environmental parameters (for instance, macromolecular crowding,[5] natural intracellular environment,[6] and inhomogeneous distribution[7]) are often neglected. Moreover, the results from these traditional experiments show only the averaged functional aspects of enzymes,[8−10] instead of their intrinisc heterogeneity,[11] driving attention to analysis within the individual cells. Key factors governing cellular regulation, such as pH, ion concentration, and especially temperature, are vital for understanding enzyme kinetics. Along with variances in enzyme activity, fluctuations in temperature also affect behavioral, morphological, biochemical, and genetic processes within a cell.[12,13] Therefore, accurate determination of cellular kinetics at various temperatures is of great importance when elucidating the functions of enzymes.

In humans, alkaline phosphatase (AP) is found in all organ tissues, with higher concentrations in bone, the liver, the bile duct, the kidneys, and the placenta. It is an essential enzyme in the dephosphorylation process, where it is responsible for hydrolyzing phosphate groups from many species (e.g., nucleotides, proteins, and alkaloids)[14,15] and thus, plays a crucial role in many biological processes, such as cell metabolism and genetic transduction.[16] Indeed, the activity of AP in human serum is widely used as an enzymatic marker for a broad range of diseases, which are coupled to the liver and bone.[17]

Indeed, there are some experimental examples of measuring enzymatic activity from single cells.[18,19] Some single-cell techniques allow the sample to be suspended in a flowing stream, such as flow cytometry,[20,21] while others isolated the individual cells then lyse for analysis.[22,23] Using capillary electrophoresis, it has been possible to separate and measure the activity of up to five different enzymes in single cells.[24,25] However, detailed strategies for the measurement of enzyme-catalyzed reactions within native single cells, possessing all the complex properties, and influential factors that are neglected in an extract experiment, have yet to be fully realized.

Microfluidic-based methods constitute a new category of tools for the manipulation of chemical environments at small length scales, transitioning single-cell studies to higher information

Received: August 21, 2014
Accepted: December 2, 2014
Published: December 2, 2014

   dx.doi.org/10.1021/ac5031418 | *Anal. Chem.* 2015, 87, 381−387

content platforms. With the possibility to integrate multiple functions into microfluidic devices, a broader spectrum of parameters can be studied in parallel and in sequence (e.g., bio(chemical) interaction, toxicology, enzymology, protein−protein interaction).[26] Although thermal control has been demonstrated to be possible within a microfluidic environment,[26] the application to the field of enzymology is quite minimal, especially when investigating response at the single-cell level. A technique capable of providing a full thermal-response curve of *in situ* enzymes, i.e., to titrate enzyme activity under known thermal gradients, has yet to be described. An ideal approach for exploring the effects of temperature on enzymes within single cells requires rapid temporal control of the local environment about the cells, while perfusing the cell at the microscale or even the nanoscale.

Herein, we present a calibrated method for directly probing the influence of temperature on enzymes within single living cells, by simultaneously controlling both the thermal and chemical environment. In this method, we utilize a previously described microfluidic tool, the multifunctional pipette, which is capable of generating a hydrodynamically confined zone of one aqueous environment within another, and to switch the content of this zone within 100 ms.[27] An optical fiber, connected to IR-B diode laser, directed toward the targeted cells, enables control of the thermal environment in a small localized area while avoiding heating the cells away from the flow zone.[28] We demonstrate the utility of this combination to generate five-point thermal activity curves within 200 s for AP in both single intact NG108-15 (NG) and HEK 293 (HEK) cells. This method has great potential as a simple analytical platform for investigating the role of thermal modulation on cell signaling, receptor response, and signal pathway regulation at the microscale. Moreover, this ability to modulate both the chemical and thermal environment simultaneously enables a greater number of single-cell experiments to be performed in each cell dish.

MATERIALS AND METHODS

Cell Preparation. Adherent NG108-15 and HEK 293 cells were plated at a density of ∼10 000 cells/cm^2 onto glass-bottom petri dishes (50 mm in diameter) in DMEM (Dulbecco's Modified Eagle's culture Medium) supplemented with 10% calf serum. The plated samples were incubated at 37 °C in a humidified 5% CO_2 atmosphere for a period of 24 h. Before each experiment, the culture medium was replaced by Extra Cellular Buffer (ECB) and the cells were washed three times by buffer exchange. The ECB buffer consisted of 140 mM NaCl, 1 mM $CaCl_2$, 10 mM D-glucose, and 10 mM HEPES, pH adjusted to 7.4 using 1 M NaOH.

Microfluidic Platform. Experiments were performed using a new implementation of the PDMS multifunctional pipette[27] with the ability to rapidly switch between four solutions. A detailed description of the device characteristics and operational parameters is given in the Supporting Information (Supporting Method). Briefly, the multifunctional pipette with its sharp tip can be readily positioned to a region within a cell dish, whereby three channels exit into the open volume. By adjusting the positive and negative pressures in adjacent channels, a hydrodynamically confined flow volume can be established, generating an isolated chemical environment at the tip. The multifunctional pipette, mounted into its holder, can be positioned using a conventional micromanipulator. A pneumatic control unit connected to the holder provides each well with an individual pressure, enabling computerized modulation of the solution flow. The typical perfusion area is 90 μm × 80 μm with flow rates of 4−8 nL/s. Because of the small flow rates employed, a cell within the superfusion zone experiences very little shear force (∼8 pN).

For our enzymatic study, ECB solutions supplemented with fluorescein, α-hemolysin, and enzyme substrate fluorescein diphosphate (FDP), were loaded into three of the four sample reservoirs of the multifunctional pipette. The fourth sample reservoir was loaded with ECB buffer to flush the cells. To achieve a reasonably homogeneous fluorescence distribution within the cell,[29] probenecid (4-(dipropylsulfamoyl) benzoic acid, Sigma−Aldrich AB, Stockholm, Sweden) was added to all solutions, with exception of α-hemolysin.

Laser Heating. The single-cell enzymatic process was thermally modulated by laser heating the sample via a directed IR-B laser beam. This laser heating system is comprised of a 1470-nm semiconductor diode laser (Model HHF-1470-6-95, Seminex) driven with an 8 A power source (4038 Laser Source, Arroyo Instruments), which delivers a localized beam to the sample through a 50-mm core diameter, 0.22 NA optical fiber (Ocean Optics). The exposed volume, based on typical positioning of the fiber end at a distance of 150 μm and angle of 52°, is ∼1 nL.[28] The temperature at the sample surface is modulated by changing the applied current at the laser source. The calibration of the heating system is highlighted in Calibration 1 in the Supporting Information.

Confocal Laser Scanning Microscopy and Fluorescence. Visualization of the cell samples was achieved through the use of a confocal laser scanning microscope (Leica TCS SP2 RS, Wetzlar, Germany) with a PL APO CS 40× magnification, 1.25 NA oil immersion lens. The 488-nm line of an Ar^+ laser was used to excite the product of FDP dephosphorylation (fluorescein).

Data Analysis. Fluorescence intensity curves were extracted from the confocal micrographs using the Leica LAS AF Lite software (Leica Microsystems, Wetzlar, Germany). All further analysis and fitting was performed using Matlab 2009b and the Matlab curve fitting toolbox (MathWorks, Inc., Natick, MA).

RESULTS AND DISCUSSION

Experimental Outline. Experiments were performed using a multifunctional pipette device, which has been described in detail elsewhere.[19,30] The activity of the enzyme alkaline phosphatase (AP) was monitored through introduction of the prefluorescent substrate fluorescein diphosphate (FDP) into the cell. AP hydrolyzes FDP, liberating the fluorescent product fluorescein. The enzyme activity was readily measured by following the production of the fluorescent product,[31] where justification of the appropriateness for following enzymatic rate is given in the Supporting Information (Supporting Analyses 1 and 2). The multifunctional pipette enables highly localized perfusion, which can be rapidly switched between four analytes, without a loss of species to the surrounding solution.[32] The cells were exposed to sequences of α-hemolysin (pore-forming agent), ECB buffer (wash solution), FDP (substrate), and fluorescein (permeabilization marker) (see the Supporting Information for further details). The pipette was positioned in front of each targeted adherent cell, situated within the patterned flow zone. The optical fiber was then positioned adjacent to the cell, to direct the IR-B heating. Each targeted cell experienced well-controlled exposure to both chemical and thermal environments, through modulation of exposure times and precise calibration of the thermal responses to the IR-B irradiation. An illustration of this basic experimental setup is shown in Figure 1.

dx.doi.org/10.1021/ac5031418 | *Anal. Chem.* 2015, 87, 381−387

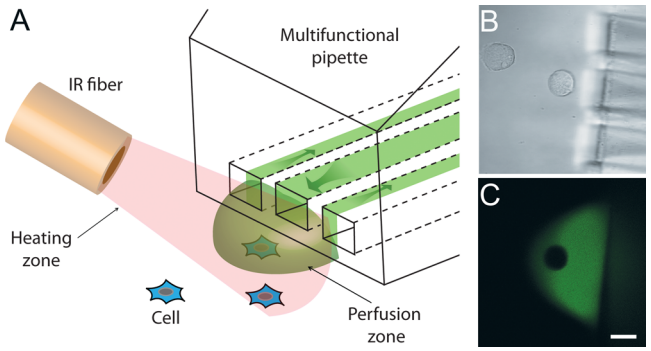

Figure 1. Illustration of an adherent cell positioned in an isolated chemical and thermal environment. (A) Schematic perspective view of the setup system, which consists of two crucial parts: the multifunctional pipette, which generates an isolated perfusion zone; an optical fiber delivering IR-B light, which creates a localized heating area. An illustration of an adherent cell being exposed in an isolated chemical environment (green) is illustrated in panel (A), whereby the cell is simultaneously being heated through exposure to the IR-B radiation (red). (B) Bright-field microscopy image of adherent cells (NG 108-15), with a multifunctional pipette tip nearby the targeted cell, with a corresponding fluorescence image shown in panel (C). Three channels exiting the tip of the multifunctional pipette enable the establishment of a hydrodynamically confined flow volume, generating an isolated chemical environment in the cell dish. In panels (B) and (C), the adherent cell close to the pipette can be exposed in an isolated chemical environment with up to four different solutions loaded into the device (10 μM fluorescein, ECB buffer, pH 7.4, was used for illustration of the flow zone). The cell has not been porated, and thus the fluorescein solution does not enter into the cell. The scale bar in panel (C) represents 15 μm.

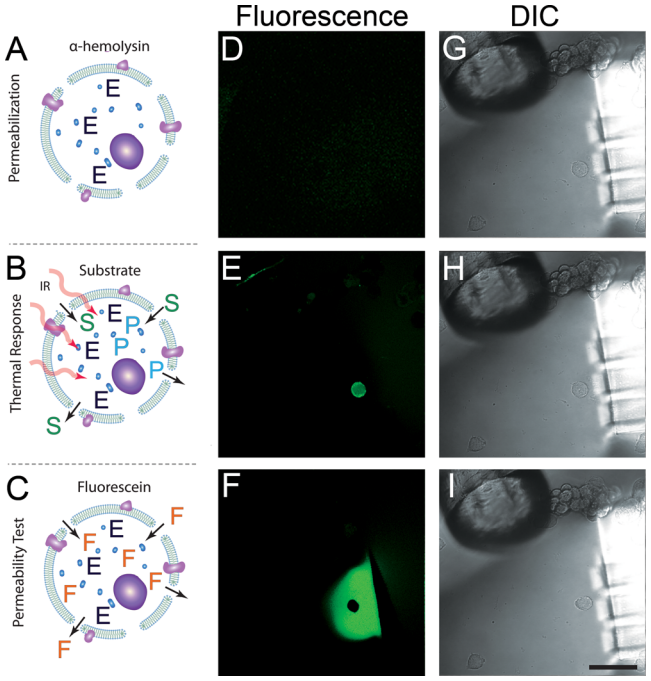

Figure 2. Experimental scheme for measuring single-cell enzymatic activity at various temperatures. Panels (A–C) show schematic illustrations representing three distinct stages in the measurement: (A) the mildly permeabilized cell is formed by exposure to α-hemolysin (200 mg/mL); (B) the permeabilized cell is exposed to the enzyme substrate (S) FDP (150 μM), while simultaneously being heated, through IR exposure to five different temperatures in sequence 22, 27, 32, 37, and 42 °C (the enzyme (E) kinetics were followed by monitoring the formation of fluorescent product (P)); (C) subsequently, the cell is exposed to 10 μM fluorescein solution to test the cell permeability. (D–F) Fluorescent images correspond to the DIC images shown in panels (G–I). Images shown in panels (D) and (G) correspond to the experimental stages in panel (A); images shown in panels (E) and (H) correspond to the experimental stages in (B); and images shown in panels (F) and (I) correspond to the experimental stages in panel (C). The scale bar in panel (I) represents 80 μm and is applicable to panels (D–I).

An example of a single-cell measurement of AP activity, from NG108-15 (NG) cells, at various temperatures, is presented in Figure 2. Briefly, the targeted cell was permeabilized, perfused with substrate during analysis, and then tested for pore closure at the end of the experiment. A schematic of the procedure is shown in Figures 2A–C; corresponding fluorescent images (Figures 2D–F) and differential interference contrast (DIC) images (Figures 2G–I) are presented for each of the stages.

To enable delivery of the substrate to the AP within each cell, pores in the membrane must be created. This was accomplished by exposure to 200 mg/mL α-hemolysin in the range of 10–20 s (see Figures 2A, 2D, and 2G), followed by exposure to the buffer for 20 s to stabilize the plasma membrane pores. The mildly permeabilized cell was then exposed to the substrate, 150 μM FDP, and discrete thermal environments were established about the target cell (22, 27, 32, 37, and 42 °C), using infrared (IR) heating, to obtain quantitative temperature-response data for alkaline phosphatase. The fluorescent response (due to the buildup of fluorescein within the cell) was monitored via confocal microscopy, as a linear increase (see Figures 2B, 2E, and 2H). At the end of each experimental run, the health of the cell, or more specifically the membrane, was interrogated by exposure to fluorescein solution for 30 s (see Figures 2C, 2F, and 2I).

Single-Cell Titration. An example of AP activity within a NG cell under various temperatures is shown in Figure 3. The fluorescence and DIC images are presented to visualize both the cell and the intracellular product buildup (see Figures 3A and 3B). The initial enzyme activity was measured at a resting state (room temperature, 22 °C), and then the poration and product formation was initiated until the fluorescence intensity rapidly increased. The temperature was then increased to 27, 32, 37, and 42 °C in sequence. The residence time at each elevated temperatures was ~40 s. The activity of the enzyme was extracted from the slopes of the fluorescence response curve, as the intracellular product concentration is directly proportional to the rate of product formation.[29] (See Calibration 2 and Supplementary Analyses 1 and 2 in the Supporting Information for details.) The enzyme activity was extracted from fluorescence region of interest (ROI) analysis, using the mean value from each cell. The data extracted from each ROI is plotted in Figure 3C.

Note that the measured enzyme kinetics are directly related to the cell permeability,[29] because of the controlling effect on the convective flow of molecules, both of the substrate and the product. Conversely, the fluorescence emissions of most fluorophores are sensitive to temperature, and can even be used as thermal monitoring dyes, such as Rhodamine B. To remove the effect of cell permeability and temperature, calibration studies were performed on known concentrations of product delivered into the cell. Within our experimental temperature range and extent of poration, <3% variance was monitored, and the effects were therefore ignored, as shown in Calibration 2 in the Supporting Information.

Enzyme Thermal Response. To investigate the effects of the cellular environment on the thermal response of AP, two

dx.doi.org/10.1021/ac5031418 | Anal. Chem. 2015, 87, 381–387

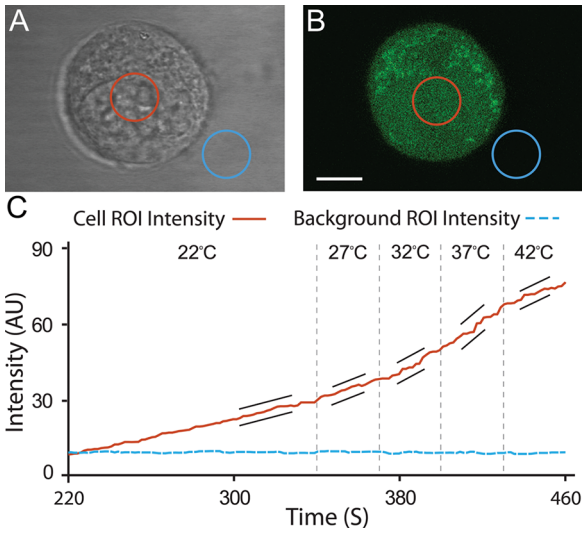

Figure 3. Investigation of AP activity within single cells at varying temperatures. The regions of interest (ROI) in (A) DIC and (B) fluorescent images labeling with red and blue ROIs represent cellular response and background, respectively; the responding curves in panel (C) show the changes the fluorescence intensity of intracellular and extracellular regions. A typical analysis of a single cell is displayed in panel (C): the blue curve extracted from the blue ROI in (B) represents the changes outside the cell; the red line from the red ROI in panel (B) indicates the fluorescence intensity from within the cell. From 220 s to 340 s, the reaction of FDP and AP initializes and the intensity due to product formation increases rapidly over the substrate background concentration. From ~340 s, the cell is exposed to localized heating with increasing temperatures of 27, 32, 37, and 42 °C for typical residence times of 30 s at each temperature. Black lines drawn on both sides of the red curve represent the slopes in those regions for the corresponding calculations. Scale bar = 10 μM.

different cell lines were used: NG108-15 and HEK 293. Thermal response plots for AP activity within individual cells are shown in Figure 4A and 4F for NG and HEK cells, respectively. Corresponding single-cell response histograms for each temperature are presented in Figure 4B–E for NG cells and in Figure 4G–J for HEK cells. The plots indicate that the enzymes have a similar trend, but not an identical response, within the temperature range of 22–42 °C, notably that the efficiency of AP in HEK cells is much higher at room temperature than in NG cells. Each analyzed cell was heated to 22, 27, 32, 37, and 42 °C in sequence, while continuously being exposed to prefluorescent substrate. The box plots present the accumulated data, where the box of the plots represents the SEM (standard error of the mean) with an n value of 30 and 16, for NG and HEK cells, respectively. The whiskers of the plots represent the minimum and maximum cell response values, and the line within the box indicates the sample median.

To identify variances within the cellular responses, enzyme efficiency distribution histograms were generated for each temperature point, with bin values of 0.1 and 0.07, for NG and HEK cells respectively, and are presented in Figures 4B–E and Figures 4G–J. The enzyme data for each cell (both NG and HEK 293) were normalized to the highest measured rate of product formation for that cell at 37 °C, treating each cell as an individual entity. To account for sample variances and to obtain a statistically representative sample, in the measurements of AP in Figures 4A–E, 30 cells in total were measured from five different cell passages, with two plated samples from each passage. For the measurement of AP activity within HEK 293 cells, 16 cells were measured from three different cell passages, with two plated samples from each passage.

The single-cell efficiency distribution plots show that the enzyme responses appear different from the two cell lines. NG cells at 22 °C have a reasonably tight clustering of efficiencies at ~40% of maximum, whereby in HEK cells, this distribution is broader and is centered closer to 60%. At 42 °C, the NG cells exhibit a more normal distribution response, shifting to lower efficiencies close to 80%, but with still quite a tight distribution, indicating no major deviation or impact on the enzyme. However, in HEK cells, the distribution changes drastically, centered at close to the same value as NG cells (~70%), but with a much more spread-out cellular response. The shape of the distributions for both enzymes has a broad range of efficiencies, which would be expected for biological samples, having various states of the cell cycle; however, the significant distribution change at 42 °C for HEK cells, and not for NG cells, may indicate that something within the NG is better able to stabilize the structure of the enzyme at elevated temperatures, shifting its efficiency peak, but not significantly skewing the distribution.

To test the ubiquity of the method a second enzyme, protease, was tested within NG cells, the results of which are presented in Figure S2 in the Supporting Information. The measured rates were in agreement with previous reports, which show the influence of temperature on AP[33,34] and protease,[35] showing that the optimum activity was observed at physiological temperatures.

Thermal Stability. Elevated temperatures can have an adverse effect on the tertiary structures of proteins, which is of particular importance to active proteins such as enzymes. To investigate any thermal denaturation of AP, a separate experimental sequence was performed, thermally cycling the cells and performing single-cell titrations, with a residence time of 20 s at each temperature point (n = 7). When the temperature was varied from 22 °C to 42 °C, an almost perfect hysteresis cycle was observed and it shows that >95% enzymatic activity can be recovered after 1 min of relaxation time, allowing the protein to refold (Figure 5A). Furthermore, the exposure time of heating was found to affect the AP activity: short exposure times (20 s) at each temperature point had little impact on the enzyme and could be cycled high temperature to low temperature multiple times in rapid succession (Figure 5B); a longer exposure time (40 s) for AP did not show the same reversible track (Figure 5C), as it remaining at a lowered activity. Therefore, the indication is that an exposure time of 20–40 s of heating could affect the active conformation of the enzyme, possibly locking it into a state that cannot be corrected within the experimental time frame.

Enzyme Analysis. Maintaining the enzyme within the cell while continuously perfusing the analyte through membrane pores can overcome two crucial issues that must be considered in enzyme studies: substrate depletion and buildup of product concentration. In this manner, cells do not need to be preincubated with dyes beforehand, allowing the enzyme–substrate reaction process to be halted until measurement determination. If only qualitative measurements are needed, the residence time for stabilizing membrane pores after permeabilization and the exposure time at each thermal point temperatures can each be reduced.[29]

The enzyme activity is ideally monitored when the product formation is at its highest rate, close to but not at, the beginning of the reaction, when the rate is directly proportional to the enzyme activity. This slower initial rate is a consequence of substrate transferring across the membrane, before it reaches a steady state. Once a steady state has been achieved, the enzyme–

dx.doi.org/10.1021/ac5031418 | Anal. Chem. 2015, 87, 381–387

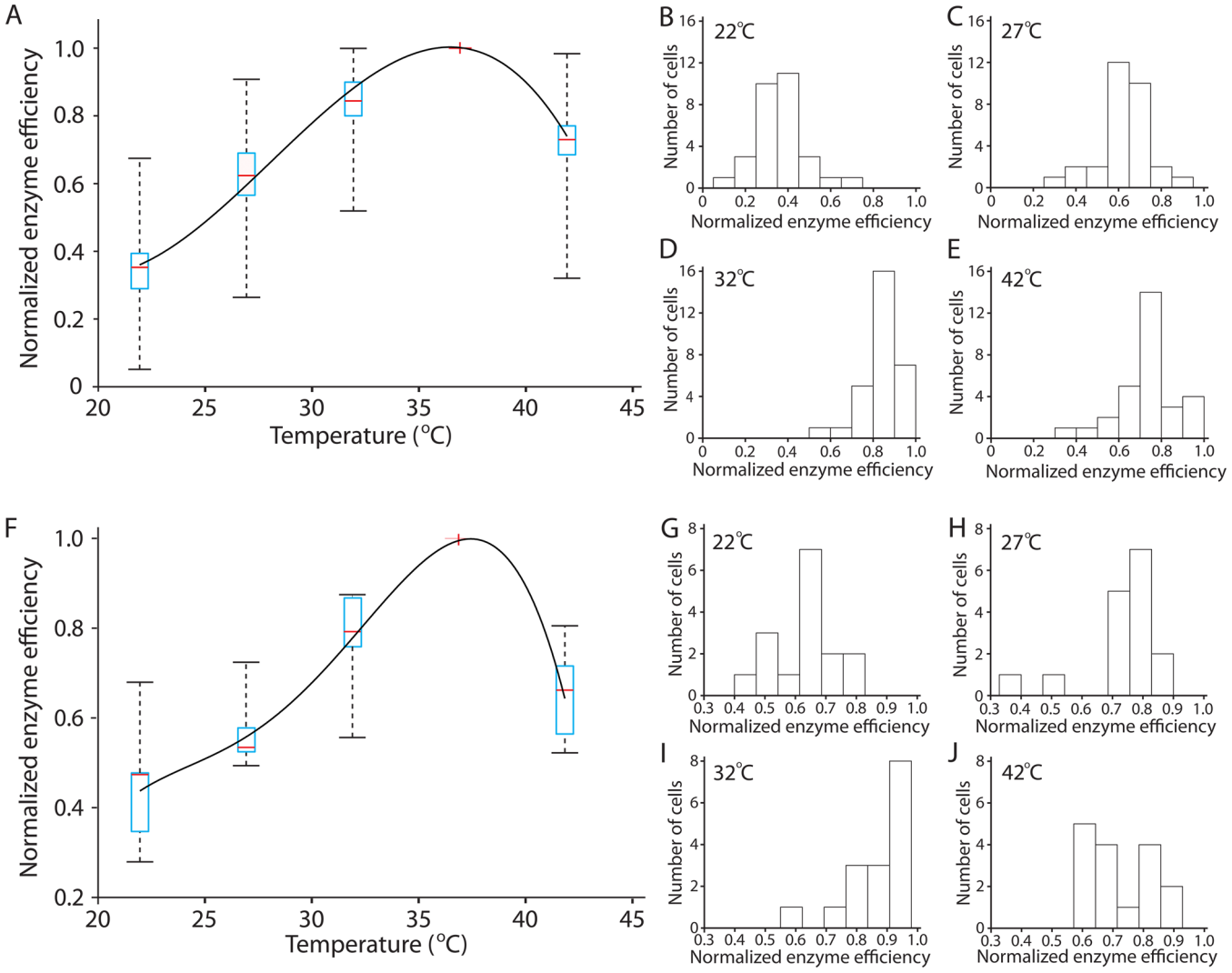

Figure 4. Thermal response plots for alkaline phosphatase (AP) activity within individual NG108-15 (NG) (A–E) and HEK 293 (F–J) cells. Each cell was heated to 22, 27, 32, 37, and 42 °C in sequence, while continuously being exposed to prefluorescent substrate. A box plot for the thermal response data of AP within NG cells is shown in panel (A), and a box plot for the thermal response data of AP within HEK 293 cells is shown in panel (F). The rectangular plots in each graph represent the SEM (standard error of the mean), with an *n* value of 30 and 16, for NG and HEK cells, respectively. The whiskers of the plots indicate the minimum and maximum cell response values, with a highlight line within the box, indicating the sample median value. Enzyme efficiency distribution histograms with a bin value of 0.1 and 0.07, for NG and HEK cells, respectively, are presented in panels (B–E) for NG cells and panels (G–J) for HEK 293 cells, for the temperature points 22, 27, 32, and 42 °C. The enzyme data for each cell (both NG and HEK 293) was normalized to the highest measured rate of product formation for that cell at 37 °C, treating each cell as an individual entity.

substrate reaction can be considered to be of zero order. Subsequently, as the enzyme active sites start to become saturated, the product formation rate will decline until reaching a plateau. This slowing of the turnover also leads to difficulty in rate extraction. As a consequence of the Michaelis–Menten kinetics, measurements can be performed at the linear-state condition for characterizing change of enzymatic activity under different temperatures (see Figure S1 in the Supporting Information).

The permeability test is a necessary step to verify that the thermal response of enzyme progress is a linear range. According to experimental observations (as shown in Figure S1 in the Supporting Information), the duration of the linear reaction response is ∼400 s for minimally permeabilized cells and ∼200 s for mildly permeabilized cells. Both are adequate times for complete multipoint response measurements. Conversely, highly permeabilized cells offer <100 s of linear range for the enzyme reaction, which is insufficient for multiple temperature points. To consider the influence of temperature on the cell permeability, a control experiment was performed to examine any changes in the cell poration level with temperature. Very little changes were observed for the temperature range of experimentation (see Calibration 2 in the Supporting Information for details).

■ CONCLUSION

We have developed a unique platform for the single-cell measurement of enzyme activity *in situ*, by locally varying the chemical and thermal environment. The approach was validated by studying alkaline phosphatase, within individual NG108-15 and HEK 293 cells, identifying differences in the AP activity between the two cell lines, potentially caused by intracellular environment differences. Unlike traditional methods for the study of enzymes, the presented single-cell platform does not require cell lysing and subsequent extraction of the enzyme, nor is it impaired by the extraction of the enzyme from the native

dx.doi.org/10.1021/ac5031418 | *Anal. Chem.* 2015, 87, 381–387

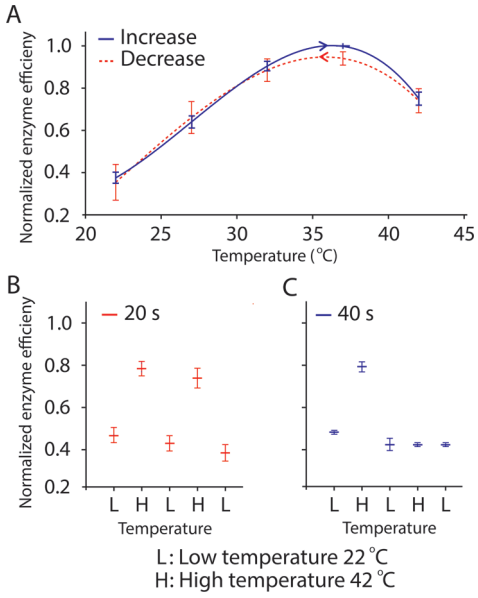

Figure 5. Effect of temperature on the stability of enzyme activity. Panel (A) shows the temperature dependence of AP activity during a thermal cycle (low → high → low). AP activity shows a hysteresis-like dependence on the temperature, if it is cyclically varied. The blue solid line and red dashed line represent the temperature increase from low to high and the temperature decrease from high to low, respectively. The temperature was held at each point for 20 s, and the data for each cell was normalized to the highest measured rate of product formation for that cell (mean ± SEM (n = 7)). Exposure duration effects on AP activity in NG108-15 cells for 20 and 40 s are shown in panels (B) and (C), respectively. The data for each cell was normalized to the highest measured rate of product formation for that cell at 37 °C (mean ± SEM (n = 7)).

intracellular environment. Instead, this method, which combines localized solution exposure using the multifunctional pipette and directed localized heating using a fiber-guided IR-B laser, achieves contamination-free exposure of single cells or small groups of cells, without solution or thermal interference to any other cells in the sample dish. The cells require no preincubation with dyes, and the membrane structure is undisturbed until the moment of permeabilization, taking place ∼20 s before initial analysis. Moreover, the cells remain in their original location without any detachment or movement during the measurement. This unique combinatorial approach enables the construction of large varying condition datasets from single-cell populations or subpopulations, aiding heterogenic identification and analysis.

■ ASSOCIATED CONTENT

Supporting Information

This material is available free of charge via the Internet at http://pubs.acs.org.

■ AUTHOR INFORMATION

Corresponding Author

*Tel.: +46 31 772 61 23. E-mail: jeffries@chalmers.se.

Notes

The authors declare the following competing financial interest(s): Gavin D. M. Jeffries and Aldo Jesorka are both founders of Fluicell AB, a company that markets the multifunctional pipette. No payments or financial gain were a reason for, or a direct consequence of, the research contained within the manuscript.

■ ACKNOWLEDGMENTS

This research was funded by the European Research Council (ERC grant), Vetenskapsrådet (VR) for G.D.M.J. and Nordforsk for A.J. and K.J. We also would like to thank Ilona Wegrzyn for the calibration of the IR heating system.

■ REFERENCES

(1) Bisswanger, H. *Enzyme Kinetics: Principles and Methods*, 2nd Revision and Updated Edition; Wiley−VCH: Weinheim, Germany, 2008.
(2) Mutch, S. A.; Kensel-Hammes, P.; Gadd, J. C.; Fujimoto, B. S.; Allen, R. W.; Schiro, P. G.; Lorenz, R. M.; Kuyper, C. L.; Kuo, J. S.; Bajjalieh, S. M.; Chiu, D. T. *J. Neurosci.* **2011**, *31*, 1461−1470.
(3) Bruggeman, F. J.; Westerhoff, H. V. *Trends Microbiol.* **2007**, *15*, 45−50.
(4) Resendis-Antonio, O. *PloS One* **2009**, *4* (3), e4967 (DOI: 10.1371/journal.pone.0004967).
(5) Schnell, S.; Turner, T. E. *Prog. Biophys. Mol. Biol.* **2004**, *85*, 235−260.
(6) Grima, R. *BMC Syst. Biol.* **2009**, *3*, 101.
(7) Murray, G. J.; Anver, M. R.; Kennedy, M. A.; Quirk, J. M.; Schiffmann, R. *Mol. Genet. Metab.* **2007**, *90*, 307−312.
(8) Sajitha Rajan, S.; Murugan, K. *Plant Physiol Biochem.* **2010**, *48*, 758−763.
(9) Malvessi, E.; Carra, S.; Pasquali, F. C.; Kern, D. B.; da Silveira, M. M.; Ayub, M. A. *J. Ind. Microbiol. Biotechnol.* **2013**, *40*, 1−10.
(10) Hao, Y. Y.; Huang, W. D.; Wu, Z.; Li, S.; Fen, Y.; Sheng, Z.; Wu, X.; Bao, X. *Zhiwu Shengli Yu Fenzi Shengwuxue Xuebao* **2004**, *30*, 19−26.
(11) Milsom, J. P.; Wynn, C. H. *Biochem. J.* **1973**, *132*, 493−500.
(12) Huey, R. B.; Kingsolver, J. G. *Trends Ecol. Evol.* **1989**, *4*, 131−135.
(13) Angilletta, M. J., Jr.; Sears, M. W.; Pringle, R. M. *Ecology* **2009**, *90*, 2933−2939.
(14) Zhao, Z.; Zhu, W.; Li, Z.; Jiang, J.; Shen, G.; Yu, R. *Anal. Sci.* **2012**, *28*, 881−886.
(15) Hoylaerts, M. F.; Manes, T.; Millan, J. L. *J. Biol. Chem.* **1997**, *272*, 22781−22787.
(16) Millan, J. L. *Mammalian Alkaline Phosphatases—From Biology to Applications in Medicine and Biotechnology*; Wiley−VCH: Weinheim, Germany, 2006.
(17) Coleman, J. E. *Annu. Rev. Biophys. Biomol. Struct.* **1992**, *21*, 441−483.
(18) Frommolt, R.; Werner, S.; Paulsen, H.; Goss, R.; Wilhelm, C.; Zauner, S.; Maier, U. G.; Grossman, A. R.; Bhattacharya, D.; Lohr, M. *Mol. Biol. Evol.* **2008**, *25*, 2653−2667.
(19) Olofsson, J.; Pihl, J.; Sinclair, J.; Sahlin, E.; Karlsson, M.; Orwar, O. *Anal. Chem.* **2004**, *76*, 4968−4976.
(20) Gao, N.; Wang, W.; Zhang, X.; Jin, W.; Yin, X.; Fang, Z. *Anal. Chem.* **2006**, *78*, 3213−3220.
(21) Baret, J.-C.; Miller, O. J.; Taly, V.; Ryckelynck, M.; El-Harrak, A.; Frenz, L.; Rick, C.; Samuels, M. L.; Hutchison, J. B.; Agresti, J. J.; Link, D. R.; Weitz, D. A.; Griffiths, A. D. *Lab Chip* **2009**, *9*, 1850−1858.
(22) Le, X. C.; Tan, W.; Scaman, C. H.; Szpacenko, A.; Arriaga, E.; Zhang, Y. N.; Dovichi, N. J.; Hindsgaul, O.; Palcic, M. M. *Glycobiology* **1999**, *9*, 219−225.
(23) He, M. Y.; Edgar, J. S.; Jeffries, G. D. M.; Lorenz, R. M.; Shelby, J. P.; Chiu, D. T. *Anal. Chem.* **2005**, *77*, 1539−1544.
(24) Meredith, G. D.; Sims, C. E.; Soughayer, J. S.; Allbritton, N. L. *Nat. Biotechnol.* **2000**, *18*, 309−312.
(25) Kovarik, M. L.; Allbritton, N. L. *Trends Biotechnol.* **2011**, *29*, 222−230.
(26) Vincent Miralles, A. H.; Florent, M.; Marie-Caroline, J. *Diagnostics* **2013**, 33−67.
(27) Ainla, A.; Jeffries, G. D.; Brune, R.; Orwar, O.; Jesorka, A. *Lab Chip* **2012**, *12*, 1255−1261.
(28) Wegrzyn, I.; Ainla, A.; Jeffries, G. D.; Jesorka, A. *Sensors (Basel, Switzerland)* **2013**, *13*, 4289−4302.
(29) Olofsson, J.; Xu, S.; Jeffries, G. D.; Jesorka, A.; Bridle, H.; Isaksson, I.; Weber, S. G.; Orwar, O. *Anal. Chem.* **2013**, *85*, 10126−10133.

(30) Olofsson, J.; Bridle, H.; Sinclair, J.; Granfeldt, D.; Sahlin, E.; Orwar, O. *Proc. Natl. Acad. Sci. U. S. A.* **2005**, *102*, 8097−8102.
(31) Telford, W. G.; Cox, W. G.; Stiner, D.; Singer, V. L.; Doty, S. B. *Cytometry* **1999**, *37*, 314−319.
(32) Boyer, M. J.; Scalarone, G. M. *Sabouraudia* **1983**, *21*, 303−315.
(33) Li, Y.; L, Y.; Liu X. Su, Z. *R. Soc. Chem.* **2014**, 42825−42830.
(34) Bano, S.; Ul Qader, S. A.; Aman, A.; Azhar, A. *Indian J. Biochem Biophys.* **2009**, *46*, 401−404.
(35) Sangeetha, R.; Geetha, A.; Arulpandi, I. *Internet J. Microbiol.* **2007**, *5* (2).

dx.doi.org/10.1021/ac5031418 | *Anal. Chem.* 2015, 87, 381−387